Chalcogenide Letters Vol. 20, No. 12, December 2023, p. 847 - 856

Characterization of undoped and doped CdS nano-thin films by ZnO for photocatalytic application

A. Thamer [a], S. Mohamed [b *]
[a]*College of Environmental Sciences Al- Qasim Green University, Babylon, Iraq*
[b]*College of materials engineering, University of Babylon, Iraq*

Using Sol-gel technology, nanocomposite CdS: ZnO thin films with an equal molar ratio of 0.5 M on a glass substrate for water decontamination purposes. The ZnO doping ratios were (0, 1, 3, 5) vol. The ultrastructural, morphological, and optical properties of the prepared thin films were studied using X-ray diffraction (XRD), atomic force microscopy (AFM), and UV-vis spectra. The results indicated that the prepared nanostructured CdS: ZnO thin films contain uniformly spaced crystalline grains of both CdS and ZnO. The ZnO-doped selection ratio and uniform grain distribution produced outstanding photocatalytic and photocatalytic performance. With a red shift in the optical band gap of CdS, the UV-Vis transmittance spectrum of the nanocomposite shows behavior that extends almost uniformly throughout the entire UV-visible region according to the near-band edge emissions of CdS and CdS: ZnO, respectively. Last but not least, the photocatalytic activity of the photodegradation of methylene blue dye was investigated and the results indicated an enhanced efficiency of approximately 87% in 60 min, much higher than that of pristine CdS: ZnO as well as CdS.

(Received August 1, 2023; Accepted December 1, 2023)

Keywords: CdS: ZnO thin films, Nanocomposite structural, Photocatalysis application, Sol-gel method, Dipping technique

1. Introduction

Environmental degradation is a major challenge that we face in the modern era. An effective method for reducing organic pollutants is photocatalysis, which uses semiconductor-based photocatalysts to remove hazardous pollutants present in the atmosphere and water [1–5]. TiO_2, CdS, and ZnO were the most popular semiconductors that are widely used as photocatalysts due to their exceptional catalytic activity, possessing sufficient band gap and photo corrosion resistance [6]. Due to its exciting high binding energy of 60 MeV [7], high electron mobility, breakdown strength, low cost, extraction stability, and non-toxic nature, cadmium sulfate attracts attention for use in this aspect. The practicality of CdS is restricted by its wide bandgap, high electron and hole formation, and low Faraday efficiency [8]. CdS is bonded to other narrow bandgap semiconductors by doping or superimposing to broaden the absorption band and, as a result, enhance the photocatalytic efficiency [9]. Due to its narrow band gap, high optical absorption, and lattice structure nearly identical to that of ZnO. ZnO is used as an impurity to improve the optical properties of CdO. ZnO and CdS have been separately realized in photocatalytic applications and have direct bulk bandgap energies of about 3.32 eV and 2.42 eV, respectively. While CdS absorbs the visible part of the radiation and thus broadens the absorption range, ZnO acts as a substrate and causes absorption in the UV range [10, 11]. Using CdS as a visible active layer improves the light absorption process since ZnO has increased carrier mobility. Due to the low excitation recombination, charge injection between ZnO and CdS results in efficient charge separation. Both are bound to ZnO and CdS, respectively [11]. These ZnO-CdS nanostructures are also believed to have easily tunable UV-Vis and photoluminescence spectra. ZnO-CdS nanocomposite is a great contender for photocatalytic applications as a result of all these elements. For the fabrication of CdS thin films, several techniques

* Corresponding author: mat.saba.mohammed@uobabylon.edu.iq
https://doi.org/10.15251/CL.2023.2012.847

have been reported, including electrodeposition [12], pulsed laser deposition [13], physical vapor deposition [14], vacuum evaporation [15], and near-space sublimation [16]. But to achieve precise control of temperature, high pressure, etc., all these technologies have complex requirements. In addition to the procedures mentioned above, Sol-gel is an easy method with low cost and accurate results. In this study, we synthesized composite CdS: ZnO nanoparticles thin films using the sol-gel process and dipping technique with different doping ratios of ZnO (1, 3, 5) volume ratio with 0.5 M of solution, and evaluated the photocatalytic activity. The structural, morphological, and optical properties of the resulting films were evaluated to understand the photolysis mechanics.

2. Materials and experimental details

2.1. Raw materials

The following were purchased from Merck: Polyethylene glycol (PEG), Cadmium acetate Cd $(CH_3COO)_2$, Thiourea (SC $(NH_2)_2$), and Zinc Acetate Dihydrate (Zn $(CH_3COO)_2$ $2H_2O$). All of the analytical-grade compounds were used directly after being received, without further purification. The entire experiment was conducted using deionized water (DI).

2.2. Preparation of CdS: ZnO thin films

First CdS solution was prepared: two solutions were prepared: the first: polyethylene glycol was dissolved in ethanol and acetic acid was added to the ethanoic solution with stirring, which continued for an hour and a half. Second: cadmium acetate and thiourea dissolved in ethanol with stirring and threading for one hour. The prepared solution 2 is mixed with solution 1 and stirred again for five hours to obtain final aqueous solubilization.

Second ZnO solution made: Pure ZnO nanoparticles were created by combining potassium hydroxide (KOH), polyvinyl alcohol, and zinc acetate dehydrate (Zn $(CH_3COO)_2$ 2H2O). (PVA). In deionized water, a 0.5 M zinc acetate dehydrate solution was created and stirred continuously for one hour. Once the solution was clear, a little amount of KOH was added in drops using a dropper until the solution took on a turbid appearance.

Third: The two solutions mixed at ZnO ratios (1.3.and 5) %vol. percentage and kept on stirring for 1 h., after this the final solution was left for three days for aged.

The final solution was deposited by dipping technique on a glasses substrate after cleaning very well. After each deposited film dry in the oven at 125 C for 15 minutes, the processer of deposition repeats three times to get the required thickness. The obtained thickness was (158.2, 154.7, 157.9, and 158.4) nm for pure and the rest of the ratios, respectively.

2.3. Photodegradation testing

The dye methylene blue (Aldrich, cap = 664 nm) was used as a probe molecule in the photocatalytic studies, which were performed in an aqueous solution. Samples were exposed to ultraviolet (A_o) light at 1 mW/cm^2 (20 W UV tube, Eurolite). The dye solution (100 mL) was stirred and bubbled with oxygen for 30 min in the dark before irradiation to allow the system to reach equilibrium and interpret chemical loss due to adsorption. Samples were exposed to light from a source that was positioned horizontally over the beaker. Using a Lambda 950 UV/Visible spectrophotometer, absorption spectra were measured at regular intervals (every 60 min) to monitor the photodegradation of the dye (Perkin Elmer). At a wavelength of 664 nm, the absorbance of MB (0.01 mM) was monitored. For all tested films, the photometric efficiency—defined as the product of the degradation rate and the incident photon flux—was determined as follows [17]:

$$\text{Degradation}\% = \frac{Co-Ci}{Co} x100 \quad (1)$$

where C_o and C_i: represent the concentration of dye in the time interval Δt,

2.4. Characterization

Using an SPM Milegra NT. MIOT, a Russian-made atomic force microscope (AFM), examined the surface morphology of the CuO: Al thin films. X-ray diffraction is used to determine the structural characteristics (cXRD). Shimadzu's XRD 6000 model uses Cuk (0.154 nm) radiation and has diffraction angles between (25° -50°). UV-visible (35-LAMBDA) is also used to measure optical characteristics.

3. Results and discussion

Fig. 1 showed the XRD of the CdS: ZnO thin film with ZnO doped were (1.3 and 5)% vol and treatment annealed at 450 °C at 2 hours. The strong peaks at 2θ = 18.25°, 26.18°, 28.61°, and 51.81° were (002), (111), (200), and (311) from the crystalline cubic phase. All specimens are cubic, polycrystalline, and well compliant with (JCPDS Card No. 89-0440) accepted [18]. The appearance of the (111) peak in the XRD pattern is evidence that cadmium has been formed. Its network constant value is set to 5.8734°. As the doping level rises, the diffraction peak strength also increases. Thus doping can promote the crystallization of CdS membranes.

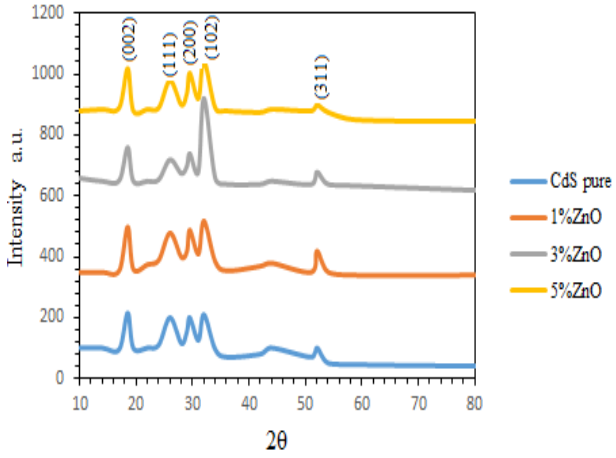

Fig 1. XRD patterns of CdS: ZnO thin films.

Also, when doping ratios rise, the full width at half maximum (FWHM) of the membranes decreases, which indicates that the grains increased after doping [19]. Using the Scherrer equation, the crystal size was calculated from the FWHM of the diffraction peaks:

$$D = k\lambda/\beta \cos\theta \quad (2)$$

When k is a constant, the shape factor is 0.94, the wavelength of the X-ray used (1.5406 °A, for CuK), the Bragg angle, and the FWHM are all given. The Williamson and Smallman formula can be used to calculate the dislocation density.

$$\delta = 1/D \ 2 \text{ lines/m}^2 \quad (3)$$

Macrostrain (ε) measured by the relation:

$$\varepsilon = \beta \cos\theta/4 \quad (4)$$

Table 1 showed the estimated values of the calculated crystalline size, dislocation density, and microanalysis. According to the XRD data, doping with ZnO causes an increase in the peak

intensity due to the reduction of the internal stress of the film and the improvement of its crystallinity.

Table 1. Structural parameters of CdS thin films.

Samples	2θ (rad)	FWHM	d-spacing	(hkl)	D (nm)	ε . 10^4 ($lin.m^{-2}$)	δ x10^{14} ($lin.m^{-2}$)
CdS	26.18	0.797	3.491	(111)	10.54	3.56	9.02
CdS:1%ZnO	26.10	0.601	3.442	(111)	13.45	2.41	7.71
CdS:3%ZnO	26.19	0.521	3.411	(111)	16.54	2.01	5.32
CdS:5%ZnO	26.21	0.432	3.400	(111)	19.12	1.58	2.89

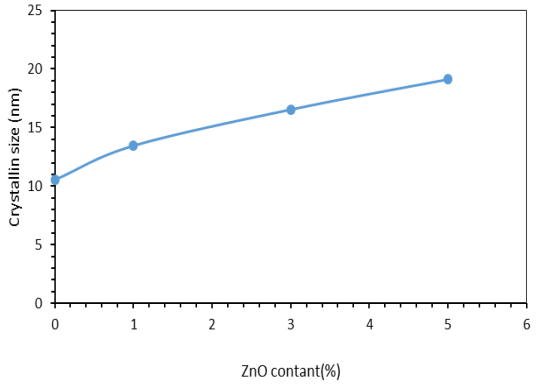

Fig 2. The crystalline size of CdS: ZnO thin films.

Doping-ZnO affects the crystal structure of CdS thin films, as doping increases the crystallite size by interfering with the CdS structure due to the difference of ionic radii between Cd (Van der Waals: 158 pm, atomic radius: 151 pm), Zn (Van der Waals: 139 pm, atomic radius: 134 pm) and S (Van der Waals: 180 pm, atomic radius: 105 pm). From Figure 2, it is seen that the crystal size increased with increasing concentration of ZnO doping, and these results are in good agreement with previously reported studies [20]. Figure 3 showed the dislocation density (δ) and total stress (ε) against the ZnO content. The density of dislocations increased with increasing ZnO doping. There is an inverse relationship between D and the rest parameters. This is due to the relationship between the density of dislocations and the size of the crystallites according to equation (2). This is value proportional to the crystallite size, and this is similar the results of the researcher (Joseph et al., 2005) [21].

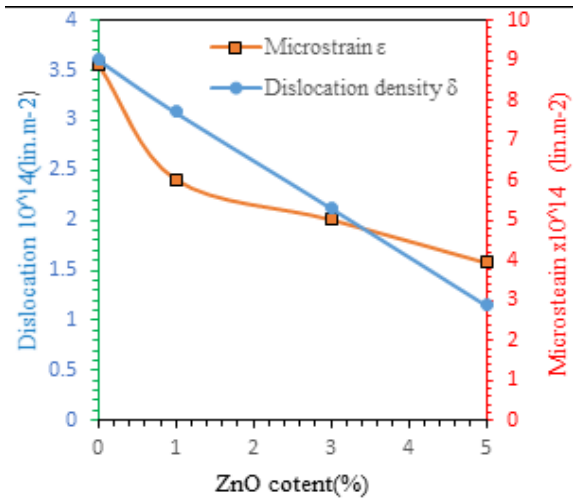

Fig. 3. Showed the dislocation density and Macrostrain of CdS: ZnO thin films.

Fig. 4 showed AFM images of CdS: ZnO thin films deposited on glass substrates with an annealing temperature treatment of 450 °C. A CdS: ZnO thin film with fine-grained morphology is seen at room temperature. The grain size distribution and surface roughness of CdS: ZnO films rise with increasing ZnO doping up to 3% ZnO, and the morphology becomes denser. Further doping to 5% ZnO leads to an increase in the grain size distribution and a decrease in the surface roughness of the CdS: 5% ZnO thin films. With increasing surface roughness, see Table 2, the FWHM value of (200) decreased at showed in the XRD data.

Table 2. AFM images parameters of CdS: ZnO thin films.

Name of samples	Roughness (nm)	Root Mea. Squ. (RMS) (nm)	Average grain size dis. (nm)
CdS pure	2.673	3.738	19.20
CdS:1%Cu	7.617	8.471	28.85
CdS:3%Cu	8.548	9.718	35.10
CdS:5%Cu	10.51	14.25	50.67

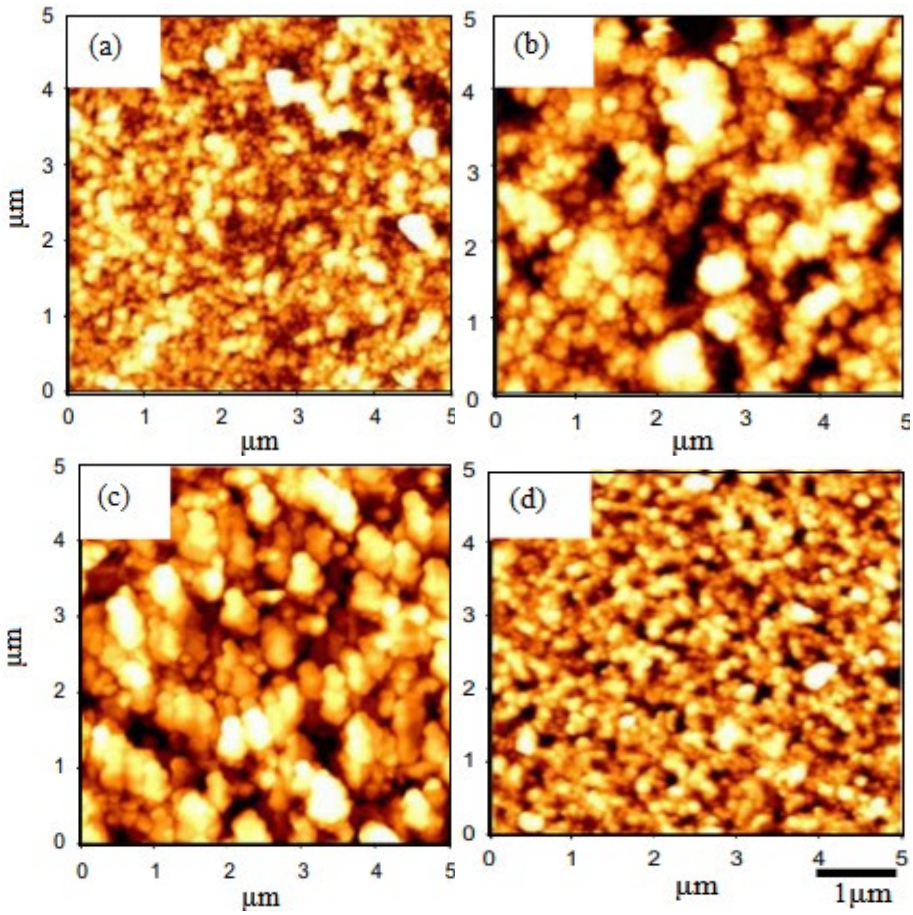

Fig. 4. AFM images of CdS: ZnO thin films:
(a) CdS pure, (b) CdS: 1%ZnO, (c) Cds: 3%ZnO (d) CdS: 5%ZnO.

In the wavelength range of 350–800 nm, the transmittance spectra of CdS and CdS:ZnO thin films were investigated. The maximum transmittance spectra for CdS:ZnO thin films range from 55% to 80%, as shown in Fig. 5. With the CdS:ZnO thin film, attenuation in transmittance is

seen in the visible wavelength range at (470–568) nm. Due to the effect of ZnO particles, the transmission edge is shifted towards a higher wavelength after doping with 5% ZnO [22]. From the Tauc equation, the absorption coefficient and optical bandgap are calculated [23]:

$$\alpha h\nu = B\,(h\nu - Eg)^{n} \tag{5}$$

where n depends on the optical transmission mode, is the absorption coefficient, eg is the band gap, and B is a constant. The value of n is 2 for transitions allowed in the direct bandgap. An extrapolation of the linear table of the Tauc equation, used to determine the optical band gap (for example) of CdS: ZnO thin films (shown in Fig. 6), is summarized in 1. It was found that with the increase of ZnO doping the energy gap decreased from (3.4 to 2.18) eV, and the results of the band gap agree with the results of (Sahay, et al., 2007) [24].

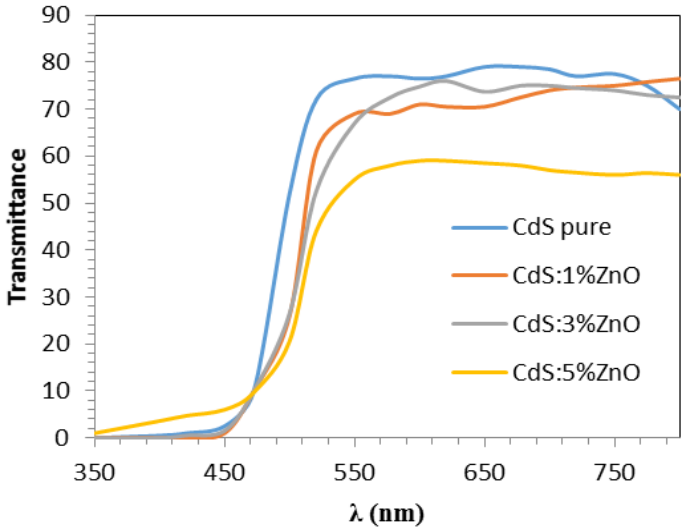

Fig. 5. Transmittance spectra of CdS: ZnO thin films.

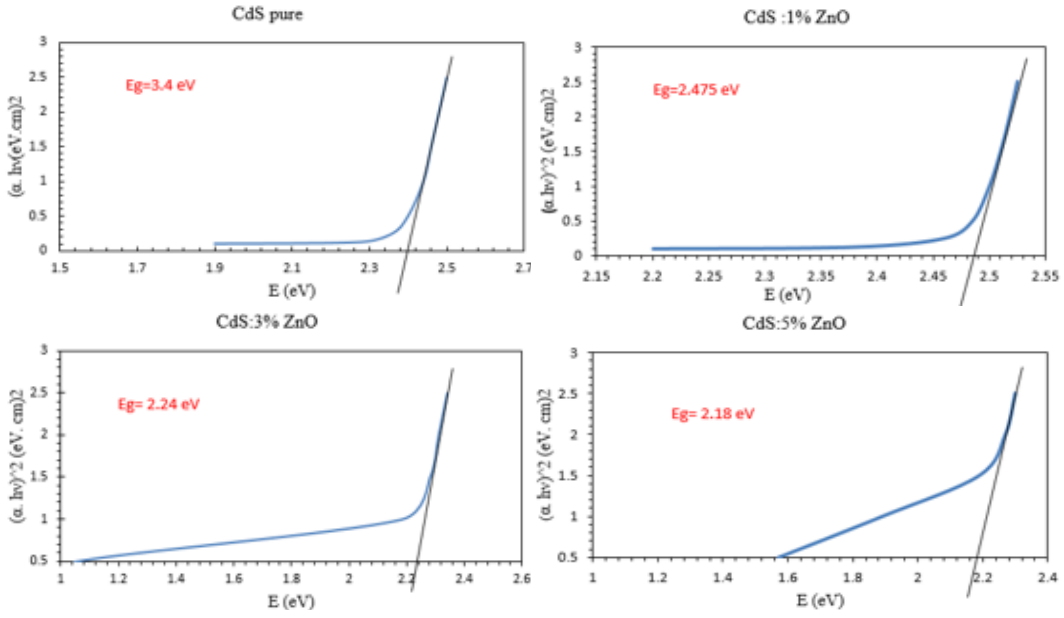

Fig. 6. The energy gap of CdS: ZnO thin films.

Using UV/visible light, the catalytic activity of CdS and CdS: ZnO thin films was studied. The contaminant used was water containing methylene blue dye. Fig. 7 shows the photocatalytic activity of CdS film and CdS: ZnO thin films over a period of 500 min at 25 °C and ultraviolet/visible light irradiation. The following equation is used to determine the photocatalytic efficiency [25]:

$$\text{Degradation\%} = \frac{Co-Ci}{Co} x100 \quad (1)$$

where Co and Ci are the initial and final concentrations of methylene blue dye before and after irradiation, respectively. Under UV and visible light irradiation, a control experiment (pure methylene blue dye) was prepared first without any catalyst, and the results showed no degradation (Fig. 7). This study shows that in the absence of a stimulus, methylene blue dye does not self-degrade under visible light irradiation, which indicates a stable behavioral pattern. When using the catalyst CdS: ZnO thin films, we notice the decomposition of the methylene blue dye under ultraviolet radiation and visible light. %. (Table 3). The table shows that the catalytic efficiency improved with the addition of impurities, as the photodegradation efficiency of methylene blue dye increased from 50% to 87% [26]. This is a consequence of the photosensitivity bands of CdS: ZnO thin films being stretched and absorbing light energy under artificial sunlight irradiation. Interestingly, the improved photocatalytic efficacy of CdS: ZnO films was often the result of charge transfer processes in CdS: ZnO thin films that prevent electron-hole pair recombination. However, the degradation kinetics of methylene blue dye was also investigated and compared quantitatively with the photocatalytic performance of the samples, and this will fit with the first-order equation [27]:

$$K_t = \ln\frac{Co}{Ci} \quad (2)$$

where kt stands for the pseudo-first-order rate constant (in min^{-1}) of early degradation.

For CdS and CdS:ZnO films, the rate constant, kt, which is the slope of the line plot of ln(C0/Ci) versus irradiation time (t) (Fig. 8), is reported as (0.0011, 0.0028), 0.0032, and 0.0041) 1 minute. This indicates that the rate constant kt of CdS:ZnO thin films was larger and was two times higher than that of CdS thin films. This indicates that the combination of CdS and ZnO resulted in a faster-than-usual breakdown of the methylene blue dye.

Table 3. Photocatalytic efficiency and rate constant of pure ZnO and CdS/ZnO.

Samples	Photocatalytic efficiency %	Rate constant k (min)
CdS pure	50	0.0011
CdS:1%ZnO	65	0.0028
CdS:3%ZnO	77	0.0032
CdS:5%ZnO	87	0.0041

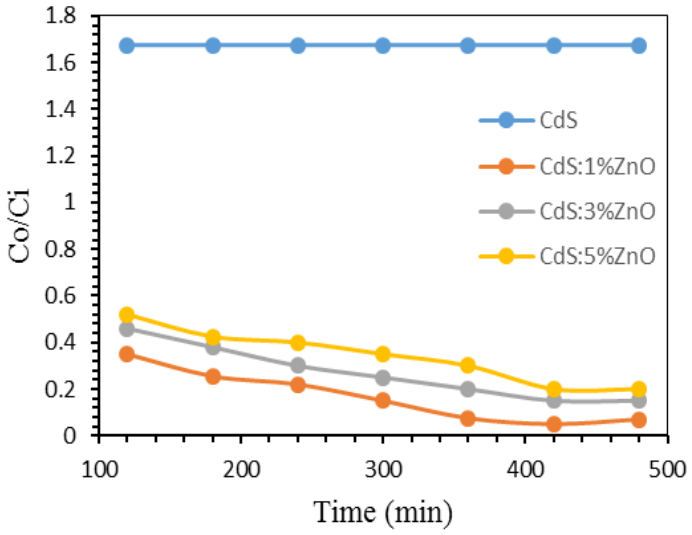

Fig. 7. Photocatalytic decomposition of dye methylene blue of CdS: ZnO thin films at different times under UV- visible light irradiation.

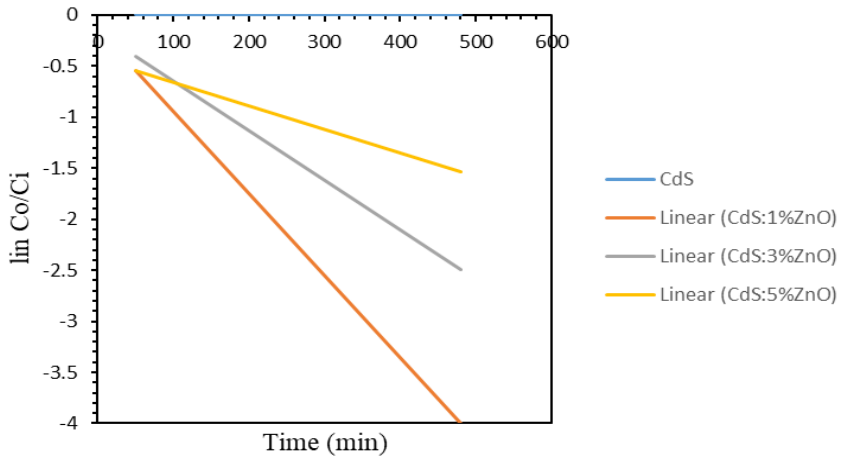

Fig. 8. The rate constants for dye methylene blue degradation of CdS: ZnO thin films at different times.

4. Conclusion

The efficient synthesis of a novel material made of CdS: ZnO thin film/glass substrate for application in heterogeneous photocatalysis to degrade an organic chemical into methylene blue is described in this study. The results witnessed a significant improvement after adding ZnO as doping and as follows:

Structure of CdS: The ZnO thin films were a polycrystalline cubic phase for all the prepared samples, and the crystal size increased from (10.54 to 19.12) nm with the increase of ZnO doped, as well as the results of dislocation density and macrostring enhancement improved with the increase in doping ratios as these values witnessed a decrease concrete.

The results of the AFM images indicate the improvement of the roughness, RMS, and grain size distribution from (2.673 to 10.51) nm, (3.738 to 14.25) nm, and (19.20 to 50.67) nm, respectively. The energy gap and optical enhancement of transmission and transmission decreased with the increase of ZnO-doped, and the energy gap also decreased from (3.4 to 2.18) eV.

Within 500 minutes, the photocatalytic activity resulted in 50-87% methylene blue breakage, and the pseudo-first-order rate constant increased from (0.0011 to 0.0014). It is possible

to use CdS: ZnO thin film as a photocatalytic to clean up industrial effluents containing other organic pollutants.

Acknowledgments

The team would like to thank the Thin Film Laboratory of the Ministry of Science and Technology/ for helping promote and sustain this work.

References

[1] M. Ding, N. Yao, C. Wang, J. Huang, M. Shao, S. Zhang, P. Li, X. Deng, X. XuNanoscale Res. Lett. 11 (2016) 205; https://doi.org/10.1186/s11671-016-1432-7

[2] X. Ke, J. Zhang, K. Dai, K. Fan, C. Liang, Sol. RRL 5 (2021), 2000805; https://doi.org/10.1002/solr.202000805

[3] Y. Huang, F. Mei, J. Zhang, K. Dai, G. Dawson, Acta Phys. Chim. Sin. 38 (2022), 2108028; https://doi.org/10.3866/PKU.WHXB202108028

[4] H. Wang, L. Zhang, Z. Chen, J. Hu, S. Li, Z. Wang, J. Liu, X. Wang, Chem. Soc. Rev. 43 (2014) 5234-5244; https://doi.org/10.1039/C4CS00126E

[5] N.U. Rehman, M. Mehmood, S.M. Ali, S.M. Ramay, T.S. Alkhuraiji, Appl. Phys. A 126 (2020) 710; https://doi.org/10.1007/s00339-020-03909-4

[6] Teng F, Hu K, Semiconductor Materials Advanced Materials 30 1-39; https://doi.org/10.1002/adma.201706262

[7] Khan Z R, Munirah, Aziz A and Khan M S, Materials Science- Poland 36 235-41; https://doi.org/10.1515/msp-2018-0028

[8] Pandya S G 2016 Influence of Growth Process on the Properties of Chemically Prepared Cadmium Sulphide Thin Films International Journal of Recent Scientific Research 7 14765-8

[9] Ikhmayies S J, Juwhari H K and Ahmad-Bitar R N, Journal of Luminescence 141 27-32; https://doi.org/10.1016/j.jlumin.2013.02.045

[10] B. Li, Y. Wang, J. Phys. Chem. Solids 72 (2011) 1165-1169; https://doi.org/10.1016/j.jpcs.2011.07.010

[11] I. Zgura, N. Preda, G. Socol, C. Ghica, D. Ghica, M. Enculescu, I. Negut, L. Nedelcu, L. Frunza, C.P. Ganea, S. Frunza, Mater. Res. Bull. 99 (2018) 174-181; https://doi.org/10.1016/j.materresbull.2017.11.013

[12] I. Zgura, N. Preda, G. Socol, C. Ghica, D. Ghica, M. Enculescu, I. Negut, L. Nedelcu, L. Frunza, C.P. Ganea, S. Frunza, Mater. Res. Bull. 99 (2018) 174-181; https://doi.org/10.1016/j.materresbull.2017.11.013

[13] M. Shohel, M.S. Miran, M.A.B.H Susan, M.Y.A. Mollah, Res. Chem. Intermed. 42 (2016) 5281-5297; https://doi.org/10.1007/s11164-015-2358-x

[14] H.M. Naeem, S. Ijaz, M.H. Abbas, Y. Ahmed, N. Rehman, T.J. Park, M.A. Basit, Mater. Chem. Phys. 252 (2020), 123190; https://doi.org/10.1016/j.matchemphys.2020.123190

[15] S. Suwanboon, P. Amornpitoksuk, P. Bangrak, C. Randorn, Ceram. Int. 40 (2014) 975-983; https://doi.org/10.1016/j.ceramint.2013.06.094

[16] K.L. Foo, U. Hashim, K. Muhammad, C.H. Voon, Nanoscale Res. Lett. 9 (2014) 429; https://doi.org/10.1186/1556-276X-9-429

[17] A. Mossad Ali, Adel A. Ismail, R. Najmye, A. Al-Hajry, Journal of Photochemistry and Photobiology A: Chemistry 275 (2014) 37-46; https://doi.org/10.1016/j.jphotochem.2013.11.002

[18] Mariappan R., Ponnuswamy V., Ragavendar M, The effect of annealing temperature on structural and optical properties of undoped and Cu doped CdS thin films

[19] Khalaph, K. A., Abdalameer, N. K., & Mousa, A. Q. (2021, November). Study the physical properties of CdSe nanostructures prepared by a pulsed laser deposition method. In AIP Conference Proceedings (Vol. 2372, No. 1). AIP Publishing.

[20] Q. Lu, Z. Wang, J. Li, P. Wang, X. Ye, Nanoscale Res. Lett. 4 (2009) 646-654; https://doi.org/10.1007/s11671-009-9294-x

[21] B. Joseph, P. Manoj, V. Vaidyan, Bull. Mater. Sci. 28(2005) 487-493; https://doi.org/10.1007/BF02711242

[22] Mohsin, A.K.; Bidin, N., In Advanced Materials Research; Trans Tech Publications Ltd.: Zurich, Switzerland, 2015; https://doi.org/10.4028/www.scientific.net/AMR.1107.547

[23] Murbat, H. H., Abdalameer, N. K., & Brrd, A. K. (2018). Effects of Non-Thermal Argon Plasma Produced at Atmospheric Pressure on the Optical Properties of CdO Thin Films. Baghdad Science Journal, 15(2), 0221-0221.

[24] Sahay, P.P.; Nath, R.K.; Tewari, S., Cryst. Res. Technol. J. Exp. Ind. Crystallogr. 2007, 42, 275-280; https://doi.org/10.1002/crat.200610812

[25] K. Adesina Adegoke, M. Iqbal, H. Louis, O. Solomon Bello, Materials Science for Energy Technologies 2 (2019) 329-336; https://doi.org/10.1016/j.mset.2019.02.008

[26] M. Iqbal, A. Ali, N.A. Nahyoon, A. Majeed, R. Pothu, S. Phulpoto, K.H. Thebo, , Mater. Sci. Energy Technol. 2 (2019) 41-45; https://doi.org/10.1016/j.mset.2018.09.002

[27] S. Min, Y. Lei, H. Sun, J. Hou, F. Wang, E. Cui, S. She, Z. Jin, J. Xu, X. Ma, Mol. Catal. 440 (2017) 190-198; https://doi.org/10.1016/j.mcat.2017.07.023